

기계 조인트의 전단 컨택 특성 측정 Measurement of Shear Contact Characteristics on Mechanical Joints

이철희†
Chul-Hee Lee

Key Words : Mechanical Joints(기계 조인트), Bolted Joint(볼트 조인트), Shear Contact Stiffness(전단 컨택 강성), Contact Damping(컨택 댐핑)

ABSTRACT

An experimental method based on contact resonance is developed to extract the contact parameters of mechanical joints under various clamped conditions. Mechanical joint parameters of shear contact stiffness and damping were extracted for different physical joint parameters such as surface finish of the mating surfaces, the presence of lubrication, the effect of the clamping pressure, and shear load. It was found that the shear contact stiffness values decreased with increasing clamping load and increased with increasing shear loading. Contact damping ratio values were almost constant with clamping load, but decreased with increasing shear load. Moreover, rough surfaces exhibited the highest shear stiffness and contact damping compared to smooth surfaces.

1. Introduction

Mechanical joints are indispensable and common components, and provide coupling forces and moments between connected structures as well as localized energy dissipation when load is applied. Although joints and contacts are common in practical engineering applications, there are certain aspects of their dynamics, such as sensitivity to interfacial parameters (e.g., contact stiffness, contact damping). It is generally understood that joint modeling, especially using physics-based models, is difficult due to the complex physical phenomena involved in such interfaces; e.g., micro- and macro-slip between the connected structures, strong nonlinearities due to micro-impacts caused by looseness of joint connections, and sensitivity to interfacial parameters.

Important phenomenon of dynamic behavior related to joint interfaces is the coupling between normal and tangential motions and forces. For example, Serpe (1) developed an experimental methodology to measure the contact stiffness and contact damping of rough surfaces using a contact resonance method. They reported that contact stiffness values increase with increasing normal load, which were also in agreement with modeling results based on the contact of rough surfaces. Using a similar idea, Hess and Wagh (2) extracted surface roughness parameters from contact resonance measurements, and Shi and Polycarpou (3) successfully measured contact stiffness and damping for various interfaces which favorably compared with both Hertzian (spherical contacts) and nominally flat rough contact surface theories.

The contact resonance method for measuring contact

stiffness and contact damping is an indirect method, as it measures some parameters which are directly related to the contact stiffness and/or contact damping through some known dynamic system model. A key in such methods is to know precisely the system dynamics of the apparatus under the conditions to be investigated. Once such parameters are measured, the contact stiffness and contact damping can readily be obtained based on the known dynamic model. A direct method based on the definition of contact stiffness has also been used to extract contact stiffness values at the micro scale.

In this paper, the measurement of shear contact properties is conducted based on the resonant frequency method. The apparatus employed for these measurements is capable of measuring both shear stiffness and shear contact damping under variable clamping and shear loading conditions. The apparatus was designed and constructed so that its dynamic response is very simple up to the frequency range of interest. This enables the shear contact stiffness and damping to be unambiguously obtained.

2. Experiments

2.1 Experimental Setup

Contact stiffness measurements using static direct load-displacement methods are difficult because the displacements involved are very small. An alternative method for measuring both contact stiffness and contact damping is based on measuring the contact resonance of the system. An experimental apparatus based on the resonance method was developed to measure the interfacial contact stiffness and damping.

Fig. 1 shows a schematic diagram of the experimental apparatus that consists of a rigid frame, a loading/locking mechanism on the top, and the fully isolated (via soft tube springs) joint assemblies to be measured. The apparatus satisfies the following design considerations:

† 책임저자; 인하대학교 기계공학과
E-mail : chulhee@inha.ac.kr
Tel : (032) 860-7311, Fax : (032) 868-1716

a) uses soft springs (k) to isolate the interface joint dynamics from the rest of the structure, b) masses m_1 and m_2 were designed such that the measured natural frequencies are in the range of 200-10,000 Hz, which is convenient to measure with conventional accelerometers, c) the structural parts of the apparatus were designed so that their natural frequencies are outside the frequency range of interest, d) loads are applied in both the shear and normal directions, and e) accessibility of acceleration and load measurements in the vicinity of the joint. The applied clamping load is controlled with a precise torque meter and converted to the corresponding normal bolt pre-load. The shear load is measured using a piezo type force transducer that is directly attached to the lower tube spring. Using this apparatus, one can measure the interfacial shear contact stiffness and damping ratio in joint structures based on the resonance response.

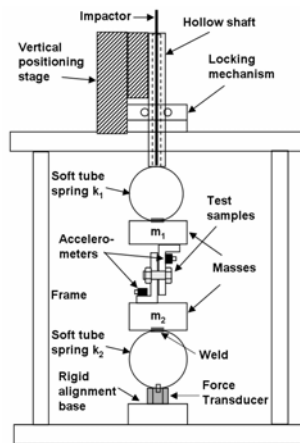


Fig. 1. Schematic diagram of mechanical joint apparatus.

In order to evaluate the effect of joint interface surface roughness, two surfaces with different roughness values were prepared; one being composed of smooth super-finished surfaces ($R_q = 0.061 \mu\text{m}$), and the other being rough surfaces with fine machining ($R_q = 1.154 \mu\text{m}$). Table 1 shows the material properties of the specimens and also the extracted surface roughness parameters. The bulk hardness values for the aluminum specimens were measured using a micro Vickers hardness tester, and their values are 117.5 H_v (or 1.15 GPa). The samples to be tested were attached to the top mass m_1 and bottom mass m_2 using rigid connections to avoid the introduction of additional compliance in the system. A one μm resolution micrometer was used to align the holes on the samples for the bolt(s) and also to exert the shear loading by control of the vertical position of the top mass. Once the sample holes were aligned, a bolt was used to secure the samples together. Also, the vertical position of the top mass was locked in place, thus isolating the nonlinear and unknown dynamics of the micrometer. Shear loading was applied by the micrometer and was controlled/measured using a piezoelectric force transducer located at the bottom of the apparatus. Once the samples were in place, an

impact was exerted on the top mass using a sharp impactor.

2.2 System Dynamic Model

In order to analyze the experimental data, a lumped parameter system model with two degrees-of-freedom was developed to represent the apparatus. For this case, the system dynamic equations of motion in the shear load direction can be written as:

$$M_1 \ddot{x}_1 + c_t (\dot{x}_1 - \dot{x}_2) + (k_1 + k_t) x_1 - k_t x_2 = F \delta(t) \quad (1a)$$

$$M_2 \ddot{x}_2 + c_t (\dot{x}_2 - \dot{x}_1) - k_t x_1 + (k_2 + k_t) x_2 = 0 \quad (1b)$$

where the viscous damping terms from the tube springs c_1 and c_2 are assumed to be negligible so that only the shear contact damping c_t contributes to the overall damping. Each mass consists of the rigid mass and the mass of each side of the joint, as shown in Fig. 1. Solving Eq. (1) for the shear contact stiffness, its value is a complex number and is given by:

$$k_t = \frac{M_1 M_2 \omega_t^4 - (M_1 k_2 + M_2 k_1) \omega_t^2 + k_1 k_2}{(M_1 + M_2) \omega_t^2 - (k_1 + k_2)} - j c_t \omega_t \quad (2)$$

When contact damping, c_t is nonzero, the root of the characteristic equation ω_t is a complex number. Since the effect of damping on the contact stiffness is small, we are interested in the absolute value of k_t ; thus, in this work, the effect of contact damping on the calculation of k_t is ignored, and the tangential stiffness is taken as the magnitude of Eq. (2). Based on the acceleration measurements from an impact experiment, one can readily extract the resonance frequencies (i.e., ω_{t1} , ω_{t2}), and the contact damping ratios, using either time or frequency domain techniques (4). In this work, a time-domain technique known as the Eigensystem Realization Algorithm (ERA) is used to extract the tangential contact resonances and damping ratios directly from the acceleration measurements.

3. Results and Discussion

3.1 Shear Contact Characteristics

The roughness parameters are listed in Table. 1. Both samples were machined ground and then polished with grit paper to obtain different roughness properties.

Table 1 Material properties and roughness parameters

	E (GPa)	H (GPa)	R_a (μm)	R_q (μm)
Sample 1 (Smooth)	72	1.15	0.061	0.081
Superfinishing				
Sample 2 (Rough)	72	1.15	1.154	1.628
Fine machining				

To perform an experiment, each joint was attached to the upper and lower mass blocks using the set screws, and then advanced downward via the 1 μm resolution micrometer. Once the bolt holes in the samples were aligned, either one or two bolts were inserted and clamped with the desired torque using the precise torque wrench. Once the desired clamping (and shear) loading were obtained, the upper system that holds the joint

structure was locked in place to eliminate the compliance and the presence of any nonlinearity in the micrometer assembly. Then, using the impactor, an impact was applied on the back side of the upper sample and the two acceleration signals were digitally recorded on a computer. At each experimental condition, 10 impact experiments were performed and averaged to reduce noise effects. Analog filters were also used to band-pass filter the acceleration signals from 10 Hz to 10 kHz.

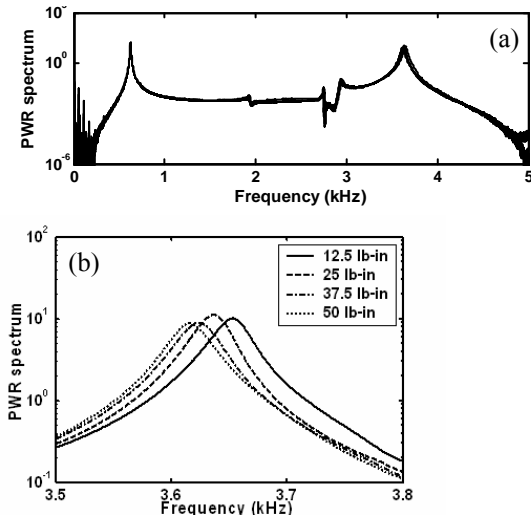


Fig. 2. Experiments for the smooth interface with changes of clamping loads: (a) logarithmic power spectrum, (b) zoomed logarithmic spectrum showing the shear contact resonances.

A typical measured acceleration response under an impact excitation is shown in Fig. 2(a). In all experiments performed in this work, the maximum acceleration was about 10 g, ensuring a sufficiently large impact excitation to excite the rigidly bolted joint structures. Fig. 2 shows the average spectra in logarithmic scale for four different clamping load experiments. The spectra contain two distinct peaks, the lower one associated with the compliant system tube springs and the higher one with the shear contact resonance in the joint structure. The resonance frequencies ω_{t1} , ω_{t2} , and the shear contact damping ratio ζ_t were extracted directly from the acceleration signals after averaging and the contact stiffness values at each clamping load were then calculated using Eq. (2). As expected, the first resonance is fixed at 612 Hz and the second resonance is slightly changing depending on the clamping load. In the case shown in Fig. 2 (smooth interface), the change in the shear contact resonance with clamping load varies from 3,632 Hz for 12.5 lb-in (corresponding to a normal pre-load of 2,491 N) to 3,602 Hz at 50.0 lb-in (normal pre-load of 9,894 N). Based on these results, increasing the clamping force, decreases the natural frequency (and thus the shear contact stiffness), even though not significantly. This phenomenon of decreasing shear stiffness with clamping load may appear counterintuitive. However, it is in agreement with Fang et al. (5). According to (5), the softening stiffness behavior can be explained by the fact

that the effective shear stiffness decreases when increasing the clamping force as the interface is in a partially locking state under no shear loading.

For the condition described above, the shear contact stiffness values vary from 23.5 MN/m at 50 lb-in to 23.9 MN/m at 12.5 lb-in. Masuko et al. (6), measured similar shear contact stiffness by directly measuring the micro-slip, and reported values for aluminum from 0 to 150 MN/m. Thus, the contact stiffness values obtained in this work are reasonably close to (6), especially as we have used smoother surfaces and a smaller nominal contact area of 151 mm². The contact damping ratios values using ERA were also extracted. Intuitively, at higher loads, the interface is more constrained, and should result in less micro-slip, thus lower damping. However, when the load reaches some critical level, there is no obvious contact damping change with further load increase. In this work, the damping ratio at 12.5 lb-in is about the same as at 50 lb-in; i.e., $\zeta_t \approx 0.11\%$. Therefore, based on these experiments, it can be seen that clamping loading only slightly affects both the shear contact stiffness and damping.

Fig. 3 shows experimental results under a constant clamping load of 50 lb-in and three different shear loads (0 N, 50 N and 100 N). The shear force was controlled with the micrometer, and measured in-situ with the force transducer (installed below the lower tube spring). As before, the results show that the system resonance is fixed at around 612 ~ 614 Hz; and the shear contact resonance slightly increases with increasing shear load. Specifically the contact resonance changes from 3,602 Hz to 3,636 Hz when the shear load is 0 N and 100 N, respectively. Clearly, the shear contact stiffness increases with increasing shear load (even though the change is only 1 %). This finding can be explained by the same mechanism as for the varying clamping force. That is, the increment of the shear load results in the interface shifting from a partially locking state towards a fully locking state.

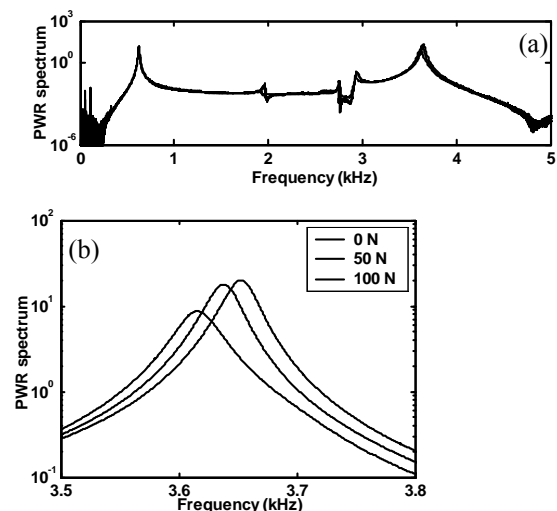


Fig. 3. Experiments for the smooth interface with changes of shear load: (a) logarithmic power spectrum, (b) zoomed logarithmic spectrum showing the shear contact resonances.

3.2 Effect of surface changes

Several specimens with different surface conditions were prepared to investigate their effect on the joint stiffness and damping. These were a joint interface with rougher surfaces obtained by machining to simulate actual joint interfaces in the mechanical structures (6). Using the same test procedure as described above, the resonance frequency results were extracted, and shear contact stiffness and damping ratio obtained using ERA, which are also plotted in Fig. 4 in terms of clamping and shear force variations. For the rough joint interface, the shear contact resonance and stiffness values are almost constant with $k_t = 24.3$ MN/m and independent of the clamping load. This finding can be explained by the same interface locking mechanism described earlier. Namely, the rougher joint interface is locked together more firmly due to the asperity roughness, unlike the smooth surface case. This also explains the phenomenon that the shear contact stiffness increases with increasing shear load. Thus, the rough surface shows higher shear contact stiffness under different clamping and shear loads compared to the smooth surface condition, which is in agreement with Ref. (6). The contact damping for the rough surface case is slightly higher than the smooth surface, and it is also slightly dependent on both the clamping load and the shear force, as shown in Figs. 4(c)-(d).

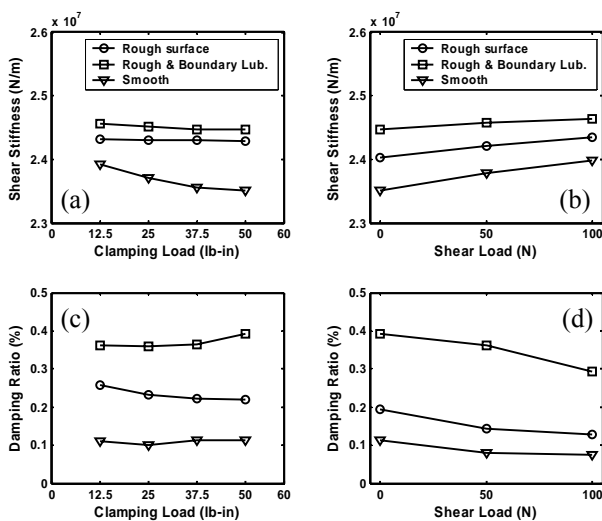


Fig. 4. Shear stiffness and damping ratio for different surface conditions under clamping and shear load changes: (a) and (c) clamping load changes (at shear load = 0 N), (b) and (d) shear load changes (at clamping load = 50 lb-in).

The small amount of lubricant simulates boundary and mixed lubrication conditions, and the results from these experiments are also depicted in Fig. 4. Referring to Fig. 4 (a) and (b), the presence of lubricant slightly increases the shear contact stiffness compared with the dry, unlubricated condition. The significance of this finding in engineering applications is that the presence of small amounts of lubricant will increase the shear contact stiffness at the joint interface. The effect of boundary

lubricant on damping is shown in Fig. 4 (c) and (d), and seems to be more dramatic, increases it to 0.4 % (from about 0.2 % in the absence of lubricant). Thus, by adding small amounts of lubricant at a joint, one can increase its damping and energy dissipation properties while maintaining high shear contact stiffness.

4. Conclusion

In this study, an apparatus was constructed to measure the shear stiffness and damping of mechanical joints using contact resonance. Based on resonance frequency measurements, one can measure the contact parameters of a joint in a clamped state. The effects of joint roughness, clamping force and shear loading have been investigated. It was found that the shear contact stiffness decreases with increasing clamping load, behaving as a nonlinear softening spring, but increases with increasing shear load for the smooth surface cases. Also, rougher surfaces show higher shear stiffness than smoother surfaces, but the rough surface with lubricant shows the highest contact stiffness. On the other hand, the contact damping is almost independent of clamping load, but decreases with increasing shear load. Thus, the shear load seems to be a source for locking the joint interface together compared with the clamping load and regardless of surface conditions. Both the shear contact stiffness and contact damping increase going from a smooth dry joint interface to a rough dry joint interface and, finally, to a boundary lubricated joint interface. An important practical finding is that a minute amount of lubricant at the joint interface significantly increases joint damping and, thus, offers improved energy dissipation in the overall structure.

References

- (1) C.I. Serpe, 1999, The role of contact compliance in the deformation, wear and elastic stability of metallic sliding rings: experiments and computational analysis, Ph.D. Dissertation, State University of New York at Buffalo, NY.
- (2) D.P. Hess, N.J. Wagh, 1995, Evaluating surface roughness from contact vibrations, ASME Journal of Tribology, Vol. 117, pp 60~64.
- (3) X. Shi, A.A. Polycarpou, 2005, Measurement and modeling of normal contact stiffness and contact damping at the meso scale, ASME Journal of Vibration and Acoustics, Vol. 127, pp. 52~60.
- (4) D.J. Inman, 1996, Engineering Vibration, Prentice Hall, New Jersey.
- (5) B.Fang, R.E. Devor, S.G. Kapoor, 2002, Influence of friction damping on workpiece-fixture system dynamics and machining stability, ASME Journal of Manufacturing Science and Engineering, Vol. 124, pp. 226~233.
- (6) M. Masuko, Y. Ito, C. Fujimoto, 1974, Behavior of the horizontal stiffness and the micro-sliding on the bolted Joint under the normal pre-load, 12th. International M.T.D.R. conf. pp. 81~88.